

1.5 Alteration Zones

Hydrothermal alteration in the area is generally characterized by intense argillization propilitization and silicification and in a few places with the introduction of gypsum-anhydrite veinlets, particularly at nearby dacite plugs.

A detailed survey was done from the Itogon bridge to Balatoc and Batuang. Altered rocks were sampled for alteration mineral identification by means of X-ray diffraction method (Table III-1-5) and petrographic analysis.

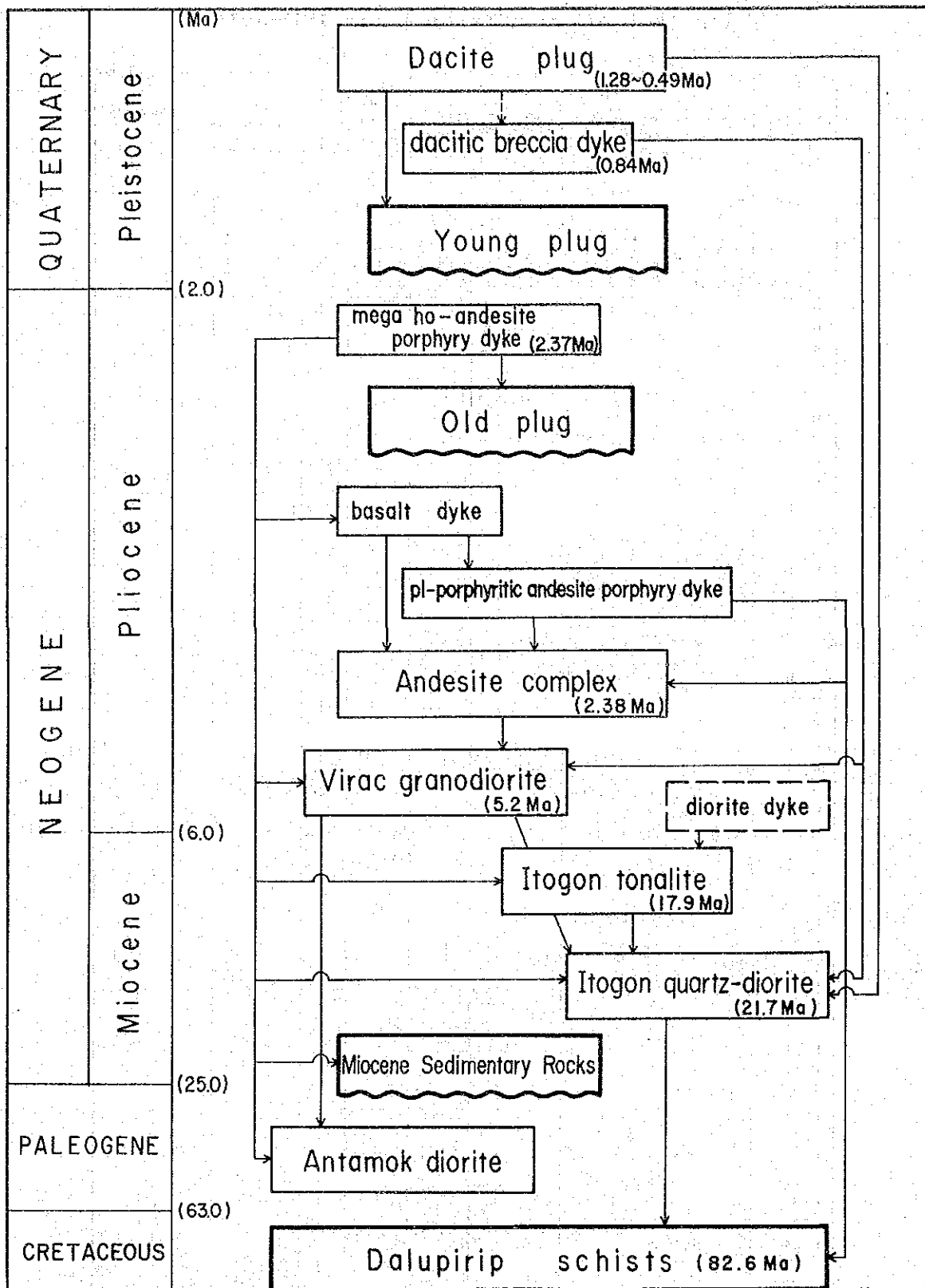
Studies reveal that the area is extensively argillized. However, some of the mineralized vein deposits observed around Balatoc and Batuang areas show quartz veins being deposited along open fractures. Some are granulated along fault zones associated with gougy materials and gypsum-anhydrite veinlets.

The alteration minerals identified were: abundant α -quartz; moderate to minor amounts of sericite; abundant to minor quantities of chlorite; minor amounts of montmorillonite; kaolinite; jarosite; pyrite; and mixed-layer minerals of sericite and montmorillonite. Other minerals identified were: meta-halloysite; chlinochlore; mixed-layers of chlorite and montmorillonite; potash-feldspar; gypsum, calcite; goethite; todorokite and magnetite. Presence of analcime, laumontite, pyrophyllite and sterco-site was uncertain.

According to the classification by Utada (1974), the hydrothermal alteration in the survey area is an admixture of:

- (i) acid-type, characterized by kaolinite and jarosite; and
- (ii) neutral-type, characterized by potash feldspar, sericite and α -quartz (Fig. III-1-6a and -b).

Neutral-type hydrothermal alteration is more widespread than the acid-type around Itogon bridge (Fig. III-1-6b). Furthermore, alteration in the Balatoc-Batuang vicinity is characterized by gypsum-anhydrite and calcite (Fig. III-1-6c).



(A → B : A intrude in B)

Fig. III-1-5 History of Igneous Activity

Table III-1-5 Results of X-ray Diffraction

Sample No.	Silicate Minerals										Sulfate minerals	Carb. m.	Oxide minerals	Note													
	Clay minerals					Zeolite minerals		Silica m.	Others																		
	montmorillonite	meta-halloysite	kaolinite	sericite	chlorite	clinochlore	pyrophyllite		sericite/montmorillonite	chlorite/montmorillonite					zeolite	analcime	laumontite	α-quartz	plagioclase	K-feldspar	amphibole	jarosite	gypsum	basanite	calcite	pyrite	geothite
H-1				Δ	Δ		?			?			⊙	⊙								Δ					
H-2				Δ	Δ					?			⊙	⊙	Δ												
H-3	Δ		Δ	Δ	Δ								⊙	⊙			Δ										
H-4	Δ		Δ	Δ	Δ								⊙	⊙													
H-5				Δ	Δ		Δ						⊙	⊙			Δ										
H-6	Δ			Δ	○					?			⊙	⊙				Δ		Δ							
H-7				○	Δ		Δ						⊙	⊙	Δ							Δ			Δ		
H-8	Δ			Δ	Δ								⊙	⊙		Δ						Δ					
H-9	Δ		Δ	Δ	⊙		Δ						⊙	⊙								Δ					
H-10	Δ			Δ	○								⊙	⊙				Δ				Δ					
H-11				Δ	○		Δ						⊙	○			Δ					Δ					
H-12	Δ			Δ	⊙								⊙	⊙	Δ							Δ					
H-13				Δ	Δ					?			⊙	⊙								Δ					
H-14	Δ		Δ	Δ	⊙		Δ						⊙	⊙	Δ							Δ					
H-15	Δ		Δ	○	⊙		Δ						⊙	⊙								Δ					
H-16			Δ	○	○								⊙	⊙								Δ					
H-17				○	○								⊙	⊙								Δ					
H-18	Δ			⊙	○								⊙	Δ			Δ					Δ				?	
H-19	Δ			Δ	○								⊙	⊙				Δ				Δ					
H-20				Δ	○								⊙	⊙								Δ				?	
H-21	Δ		Δ	○	○								⊙	⊙	Δ							Δ					
H-22	Δ			Δ	⊙								⊙	⊙								Δ					
H-23	Δ			○	⊙		Δ						⊙	⊙								Δ				?	
H-24			Δ	○	○		Δ						⊙	⊙								Δ					
H-25	Δ		Δ	○	○								⊙	⊙								Δ				?	
H-26				○	○		Δ						⊙	Δ	Δ							Δ					
H-27	Δ	Δ		○	○								⊙	Δ								Δ					
I-2				○	⊙		Δ						⊙	⊙								Δ				?	
I-3				○	Δ		Δ						⊙	⊙								Δ					
I-4	Δ		Δ	Δ	Δ								○	⊙	⊙							Δ					
I-7	Δ		Δ	Δ			Δ						⊙	⊙	Δ							Δ					Δ
I-9	Δ		Δ	Δ	○								⊙	⊙	Δ							Δ					
I-10				Δ	Δ								⊙	⊙								Δ				?	
I-13	Δ			⊙	Δ								⊙	⊙								Δ					?
I-18	Δ			○	○								⊙	○								Δ					
I-21				Δ	Δ					?			⊙	⊙	⊙							Δ					
I-22	Δ		Δ	Δ	○								⊙	⊙			Δ	Δ				Δ					
I-24	Δ		Δ	Δ	⊙								⊙	⊙								Δ					
I-28	Δ		Δ	○									⊙	Δ								Δ					
I-32	Δ			Δ	Δ								⊙	⊙								Δ					
I-34	Δ			Δ	Δ								○	⊙	○							Δ					
I-38	Δ		Δ	○	Δ								⊙	Δ	Δ							Δ				?	
I-39	Δ		Δ	Δ	Δ								⊙	Δ								Δ					
I-41	Δ		Δ	Δ									⊙	⊙	Δ							Δ					
I-45		Δ											⊙	⊙								Δ					
I-46	Δ		Δ		Δ		Δ						⊙	Δ								○					
I-50	Δ			○									⊙	Δ								Δ					
E-40													Δ									?	⊙				
F-146													Δ									?	⊙				

⊙: abundant, ○: common, Δ: rare, ?: inaccuracy.

calcite sinter
calcite sinter

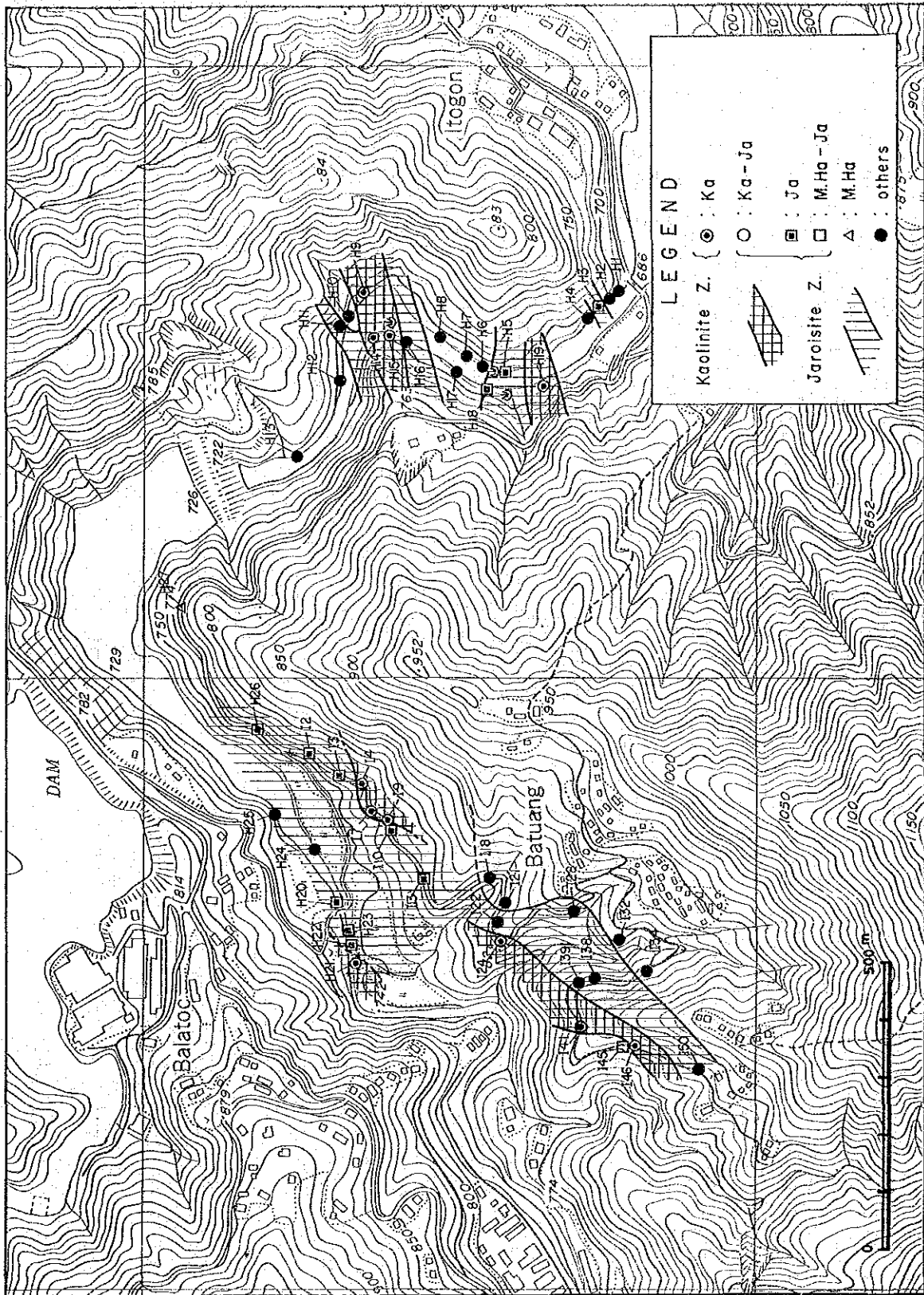
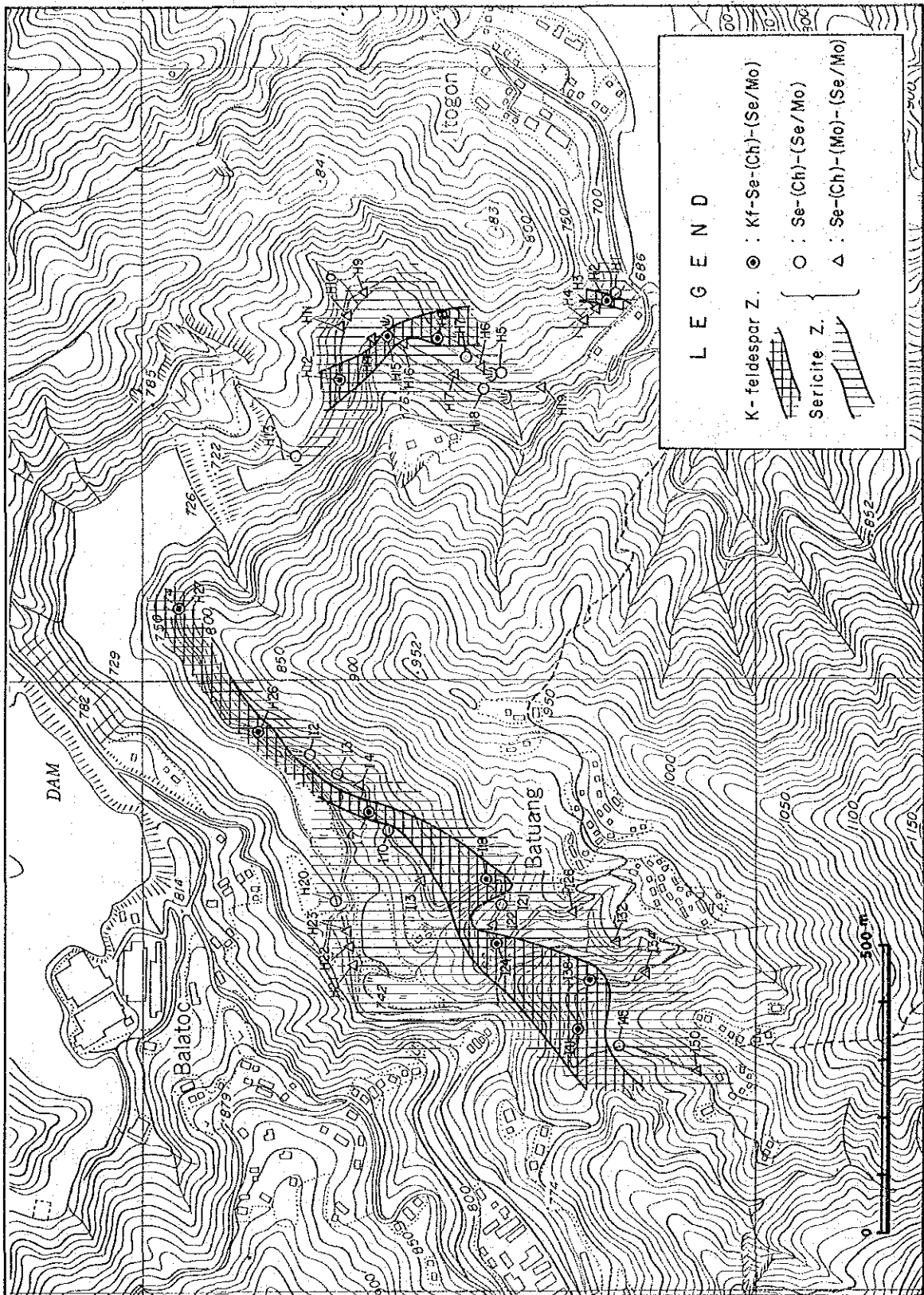


Fig. III-1-6(a) Distribution of Alteration Minerals
(Acid Hydrothermal Alteration Zone)



**Fig. III-1-6(b) Distribution of Alteration Minerals
 (Neutral Hydrothermal Alteration Zone)**

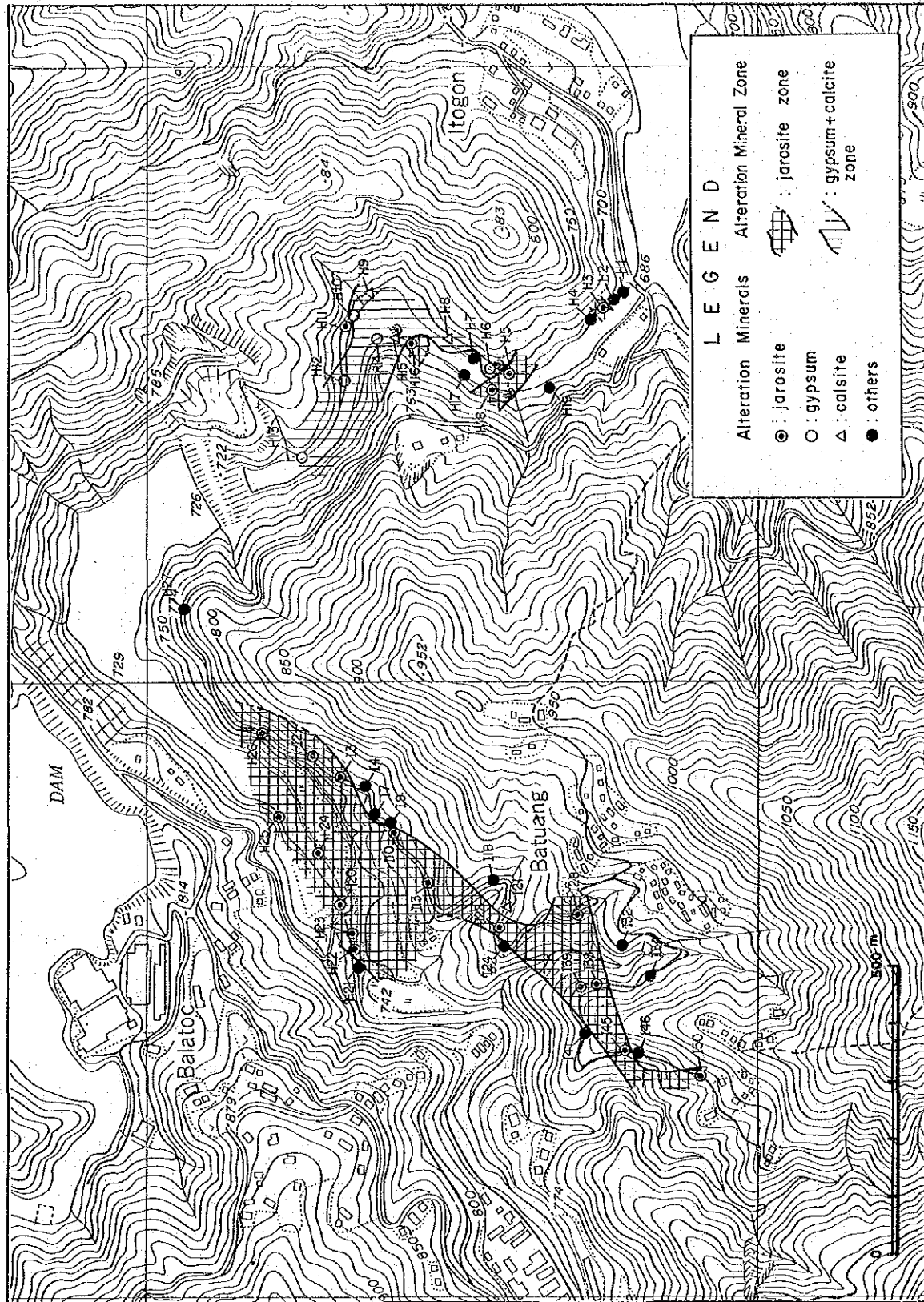


Fig. III-1-6(c) Distribution of Alteration Minerals
(Jarosite Zone and Gypsum + Calcite Zone)

Both types of alteration tend to co-exist around Balatoc and Batuang. The distribution of jarosite has widely extent (Fig. III-1-6c) and localized along the northeast southwest fractures which runs almost parallel to the gold vein system of Acupan-Itogon mine area.

1.6 Geological Structure

On a regional scale, the survey area is situated at boundary between the western side of the north-south trending central uplift zone and the eastern periphery of the west downthrown block. As mentioned before, the area is generally characterized by the intersection of the north-south, northeast-southwest and north-west-southeast faults.

Folding is also recognized in the Dalupirip schists and the Miocene Sedimentary Rocks

1.6.1 Fold Structure

In the Dalupirip schists, the anticlinal axis is north-south which runs parallel to the intrusional trend of the Itogon quartz diorite. This anticlinal structure could have been formed during the uplift of the central Cordillera by the combined effect of plutonic-Tectonic events in the past.

The northeast-southwest trending anticlines and synclines with intervals of 300-400 meters are found in the Miocene Volcano-Sedimentary Complex. The fold axes plunge to the northeast. The fold structures do not conform with the trend of intrusion of the Itogon quartz diorite. The folding of the Miocene sediments could have been formed by the later crustal movement which generated compressional stresses coming from the northwest and southeast.

1.6.2 Fault Structure

Three sets of faults are defined in the survey area: The first has north-south trend; and the second and third are conjugate fault system trending northeasterly and northwesterly, respectively.

The north-south fault system dissects the northeastern part of the area. The fracture zone (50–100 meter in width) represents the geologic boundary between the Dalupirip schist and the Itogon quartz diorite. This structural contact generally has a north-south strike. It extends to the north running parallel to the fold axis of the schist.

The northeast-southwest structures are defined in Balatoc-Acupan mine area and its vicinity. The fault strikes are parallel to the direction of the gold veins system of Acupan mine. The well defined northeasterly trending fault cutting through the Batuang area is called the 'Star Fault'. Horsetailing mineralized vein system of the Star Fault are presently being explored for gold by Benguet Corporation.

1.6.3 Fractures

Post-Pliocene andesitic dikes and quartz veins related to mineralization are observed the survey area. A fracture analysis of the structures has been undertaken.

Locations of the dikes and quartz vein identified in the geological survey are shown in Fig. III-1-7. Figs. III-1-8 and III-1-10 show the projected dikes on the Wulff net for the dikes and quartz veins, respectively. Figs. III-1-9 and III-1-11 are the Rose diagrams showing the frequencies of the strikes.

On the basis of these figures, the following prominent dip and strike for dikes are obtained: from the Wulff net, the dominant dip is 90° north-south; and from the rose diagram the prominent strikes are N70E, N40E, N50W, EW and NS.

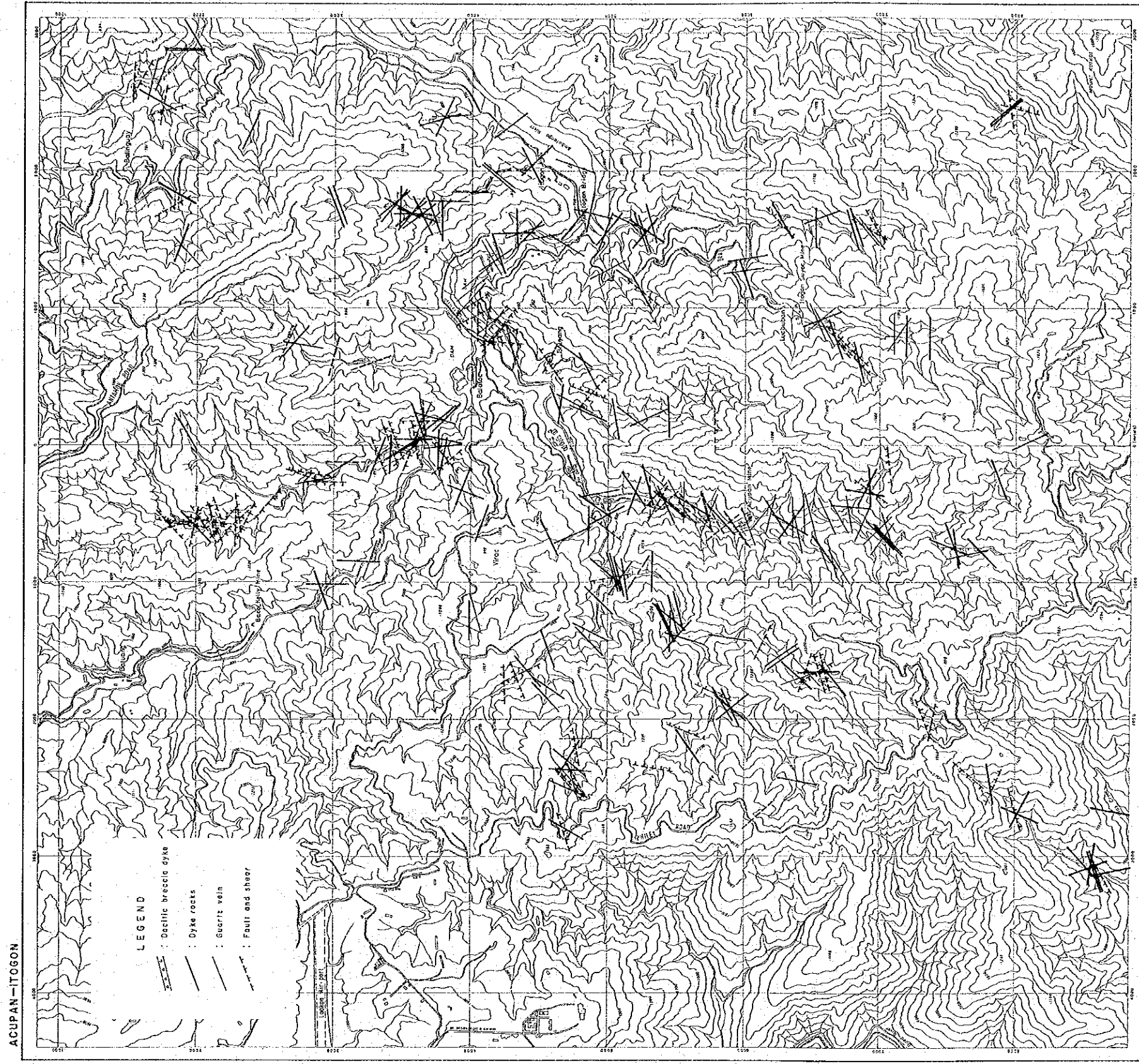


Fig. III-1-7 Distribution of Dyke Rocks, Quartz Veins and Fractures

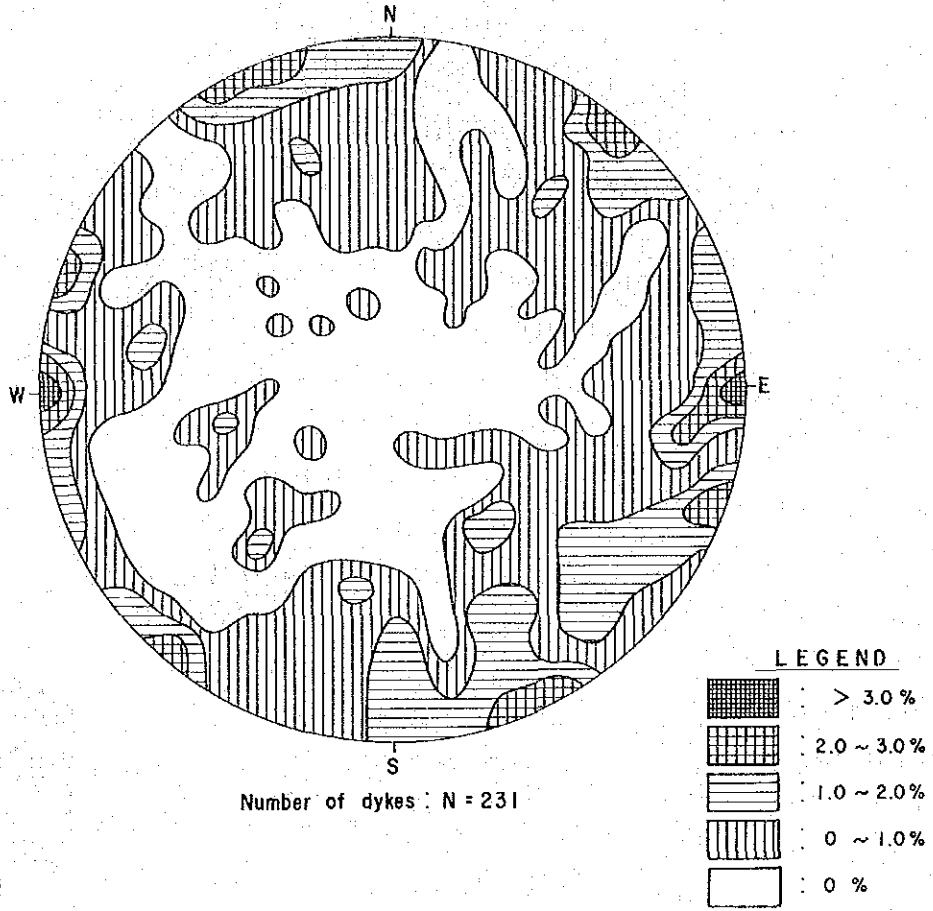


Fig. III-1-8 Frequency Distribution Diagram of Dyke Rocks

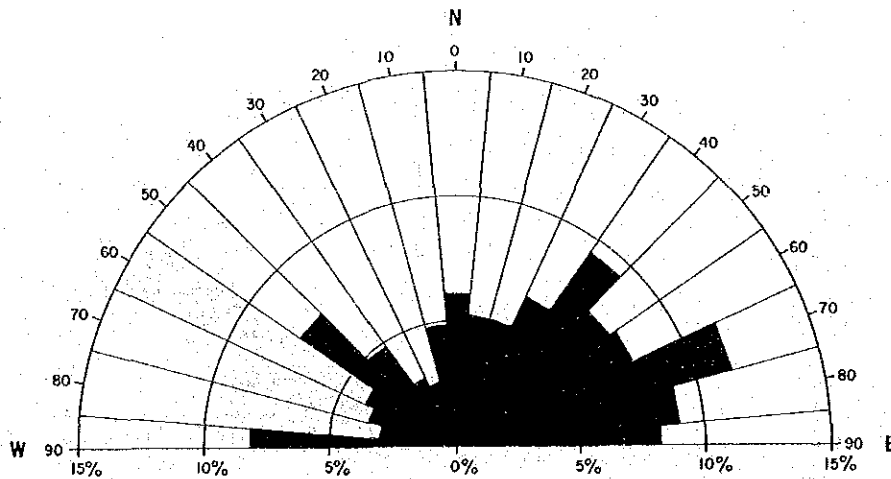


Fig. III-1-9 Rose Diagram of Dyke Rocks

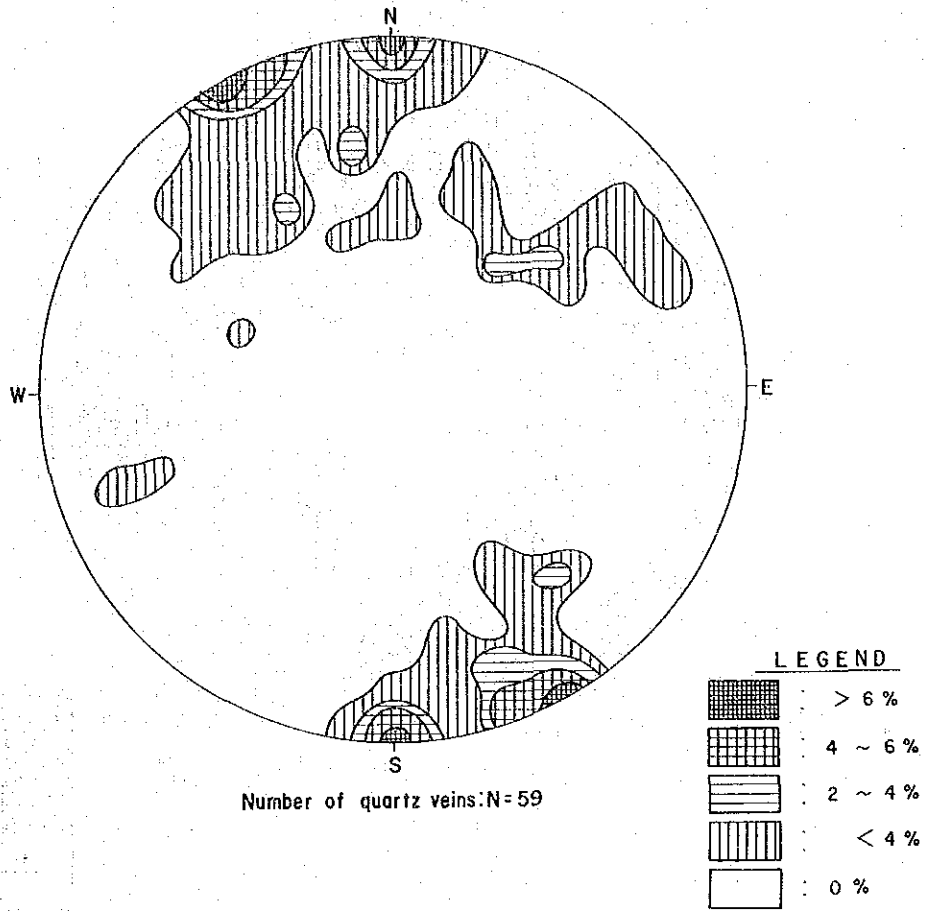


Fig. III-1-10 Frequency Distribution Diagram of Quartz Veins

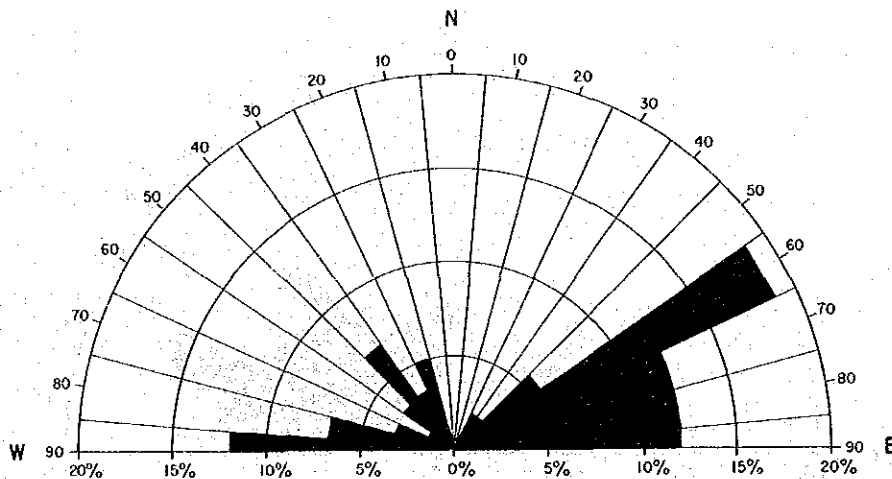


Fig. III-1-11 Rose Diagram of Quartz Veins

As to the quartz veins, prominent dip obtained from the Wulff net are almost vertical (90°); the less prominent ones range from 70° to 60° to the south. Prominent direction of the strikes obtained from the Rose diagram are $N60^\circ E$, EW, $N70^\circ E$ and $N40^\circ W$ in the order of frequency.

Assuming that these prominent directions of dikes and quartz veins reflect the basic fracture systems of the area, the estimated fracture structure is given below:

(a) The NS fracture system are estimated from the dominant trend of the dikes occurring within the central part of the survey area. The occurrence of the dikes are at intervals of 400–1000 meters. The NS trending dikes however are not very widespread in occurrence in the Itogon quartz diorite and Antamok diorite;

(b) The northeasterly fracture system cut into the Virac granodiorite and Andesite complex, which is observable within the area bounded by the dacite plugs of Acupan and Itogon. Fractures of the same system also partially extend into the Antamok diorite and Itogon quartz diorite. These fractures run parallel to the Acupan quartz-gold veins system which are generally localized around and inside the Balatoc Plug; and

(c) The northwest-southeast dikes are found concentrated mainly in the northeastern part of the survey area.

1.7 Considerations

Regional geological structure in the northern part of the Luzon Island is characterized by the NS fault block and the intersections of the conjugate northeasterly and northwesterly trending fractures. The said NS block comprises the central uplift and downthrown sections. The Acupan-Itogon area is located within the transitional zone of the central uplift and the west downthrown blocks.

The central uplift zone is composed of the Late Cretaceous Dalupirip schists, Late Oligocene Antamok diorite and Miocene Itogon quartz diorite. The west

downthrown section is underlain by Miocene Sedimentary Rocks. The Early Pliocene Virac granodiorite and Late Pliocene Andesite Complex are widely distributed at the central part of the area.

The geological setting in the area is marked mainly by north-south and northeast-southwest trending and fold structures with northeast-southwest trend. On the basis of strike frequencies of dikes and mineralized quartz veins, it may be inferred that the north-south, northeast-southwest and northwest-southeast fracture systems control the geological emplacement of the Virac granodiorite, Andesite Volcanics, dikes and plugs in Acupan area. The geological structures in the area are shown in Fig. III-1-12.

The trend of the lithological contact of the Miocene-Sedimentary Rocks exposed at the western part of the downthrown section, exhibited a north-south trend at its southern part; northeast-southwest trend at the central part; and northwest-southeast trend at the northern part. The contacts could be attributed to the structural boundary of faults having the same directions.

Based on the analysis of the faults and dikes distribution in the area, the development of significant structural network seems to be concentrated within the transition zone centrally located at the lithological boundaries between the Andesite Complex and Virac granodiorite; and the Antamok-Itogon diorite and Andesite Complex. It is inferred that the igneous activities are mainly controlled by the north-south, northeast-southwest and northwest-southeast trending fracture system as evidenced by the alignment of dacite/andesite breccia plugs found in the Acupan Mine, Itogon Bridge and along Kennon Road which are generally localized at the intersection of north-south, northwest-southeast and the northeasterly trending conjugate faults.

Similarly, the geothermal manifestations in the area such as hot springs or thermally altered grounds are closely related to the northeast-southwest faults which develop in and around the plugs. It may be said that upheavals of the central uplift zone as well as the associated structures have induced the hypabyssal intrusion of the Pleistocene dacite plug, considered as the possible heat source of the geothermal system in Acupan-Itogon prospect area.

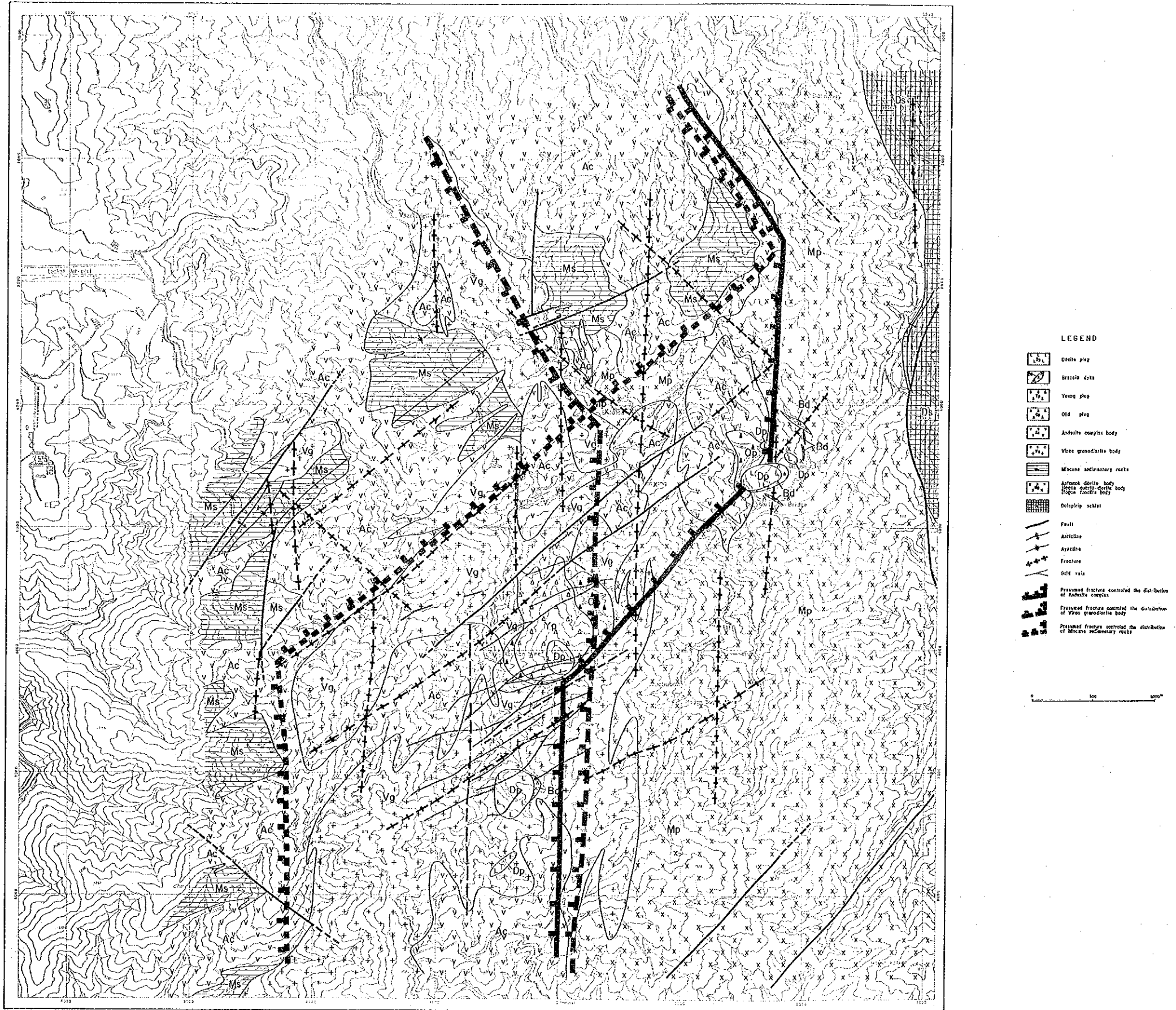


Fig. III-1-12 Schematic Tectonic Map

2. GEOCHEMICAL SURVEY

2 GEOCHEMICAL SURVEY

2.1 Purpose of the Survey

In the project Phase-I, the respective surveys and exploration were carried out on an introductory basis and the potential of such endeavors were reviewed. At the same time, existing data were gathered and the geothermal system underground was evaluated through a comprehensive analysis of those data. The purpose of the Phase-II activity was to undertake detailed geochemical survey on the delineated ten (10) kilometer square prospective area with a view of reconstructing the geochemical model of the geothermal system in Acupan-Itogon prospect. The survey includes the following:

- (a) Ground geochemical survey (199 stations);
 - soil temperatures;
 - mercury concentration in soil; and
 - radon gas concentration in soil-air.

- (b) O/H isotope analysis of hot spring water (15 samples).

2.2 Methodology

2.2.1 Ground Geochemical Survey

The survey area was grid with 250 meters spacing. Each grid station was set up along roads, ridges and creeks, and located far from artificial structures. The location of every survey station was plotted on a topographic map with a scale of 1:10,000. The elevation of each station based on the topographic map and ground control, slope, vegetation, air temperature, etc. were entered in the data sheet.

- (a) Soil temperature measurement: The method is the most direct way to detect anomalous heat flux to the surface brought about by geothermal activity underneath. Since the method is simple and economical, it is one of the exploratory

tools that have long been used. It is, however, occasionally influenced by irregular or unusual phenomena near the ground surface.

In this survey, the method was used to possibly delineate the extent of geothermal anomaly in Acupan-Itogon. At each station, the ambient temperature was measured. A hole was drilled with hand auger for the measurement of soil temperature, initially at the depth of 60 centimeters (Table III-2-1). A thermistor sensor (Type D-611) was inserted about 20-30 millimeter into the bottom of the hole and was kept standing for 3-5 minutes until the bottom temperature stabilized. The temperature indicated in the digital meter was recorded. Then, the hole was deepened to 100 centimeters and the bottomhole temperature was measured in the same manner as above.

The daily variation in the bottom temperature at the base point was monitored during the period October 6 to November 21. The effect of elevation differences upon soil temperatures was also studied.

(b) Determination of Mercury content in soil: It is generally said that the quantity of mercury in surface soil of non-geothermal field is 0.002-0.005 ppm. In the case of geothermal field, the quantity is 100-1,000 times more concentrated. These unusual figures are considered to be indications of underground geothermal fluid and a good fracture system which serves as channelway for ascending thermal fluid. However, the concentration of mercury in soil reflects the sum result of its dissipation and accumulation with time, and does not always indicate the present underground activities.

The residual soil formation is generally poor in the survey area, and as such, it was difficult to obtain samples from the A_1 horizon. Hence, sampling was carried out in bulk of more than 500 grams from a depth of 10-20 centimeters below the surface excluding the A_0 horizon (humic layer). The sampling date, sample number, soil color, dryness, size of soil particles, etc. were noted. The soil samples were put in sealed vinyl bags and were kept in a dark place. The bags were then transported to the BED laboratory in Manila where the samples were air-dried in preparation for mercury analysis.

Mercury Analysis: After the collected soil was air-dried for 1–2 weeks, sorting was made using Tyler's sieve of 80-mesh.

The following are the pre-treatments done on the samples prior to the analysis:

(i) Two (2) grams of the 80-mesh sieved sample is put in a beaker. Twelve (12) millimeter of nitric acid and sulfuric acid (HNO_3 and H_2SO_4 in the proportion of 2:1) and 5 ml. of potassium permanganate solution (5% KMnO_4) are added to the sample.

(ii) The beaker is placed in a water bath at $50\text{--}60^\circ\text{C}$ for two hours. The color of potassium permanganate is maintained by the addition of the save every time that the color disappears.

(iii) The content is cooled to room temperature and 2–3 drops of hydrozylamine hydrochloride (30% $\text{NH}_2\text{OH}\cdot\text{HCl}$) solution are added.

(iv) The solution is transferred to a 100 ml. measuring flask, and water is added to dilute the solution to the 100 ml.

(v) After shaking the flask thoroughly, the solution is filtered using No. 2 filter paper.

(vi) 10–50 ml. of the filtrate is transferred to a flask, and the total volume is made 105 ml. with the addition of water.

(vii) Ten (10) ml of reducing liquid is added to the solution, which will be used for the measurement. [To prepare the reducing liquid, 50 mg. of stannous chloride ($\text{SnCl}_2\cdot 2\text{H}_2\text{O}$) is completely dissolved in 130 ml. of sulfuric acid solution (H_2O and H_2SO_4 in the proportion of 1:1); then water is added to make the solution to 200–300 ml. and allowed to stand until it becomes clear. The solution is made up to a final volume of 500 ml. with water]. The flask containing the filtrate and recuding liquid is

set in the mercury analyzer (Hiranuma HG-1 type) and the mercury content is determined.

The following are the specifications of the analytical equipment:

Measurement method: Mercury analysis by reduction-aeration method.

Luminous source: Low-voltage mercury vapor lamp.

Luminous receiver: Photoelectric tube

Detection sensitivity: 0.005 μg .

Accuracy of repeated measurements: 3% or less

Full scale: 0.5, 1, 2, 3, and abs. 1 (five-step changeover)

Output terminal: 10 mV full scale (for recorder)

Power source: AC 100 V \pm 10 V

(c) Determination of Radon Gas

content in soil-air: Radon (atomic weight 222) is produced as alpha decay product of Radium (atomic weight 226) in the course of radioactive disintegration of Uranium (atomic weight 238). Theoretically, the origin of Radon is attributed to Radon in groundwater (Horiuchi and Murakami, 1978) or in granites (Belir, 1959; Sugihara, 1978), although its distribution is greatly influenced by variations in geological nature. Nevertheless, anomaly in Radon gas occurs immediately above the geothermal system and is controlled by fracture systems because of its short half-life and comparatively small dispersion.

The Radon track-etch cup, a product of Terradex Corporation, U.S.A., was used for the measurement of Radon gas being emitted from the ground. The cup was buried inside a hole of 60 cm. depth drilled by hand auger (Fig. III-2-2). Easily

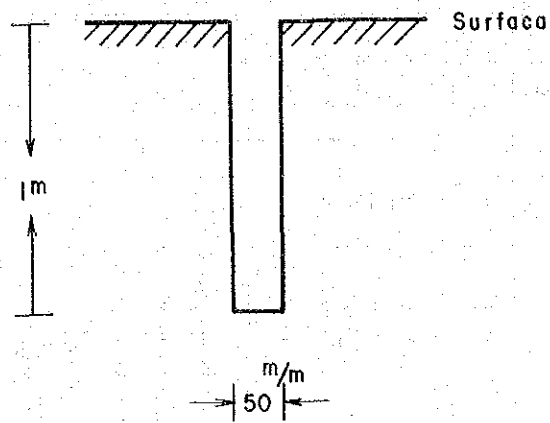


Fig. III-2-1 Profile of Hole for Temperature Measurement

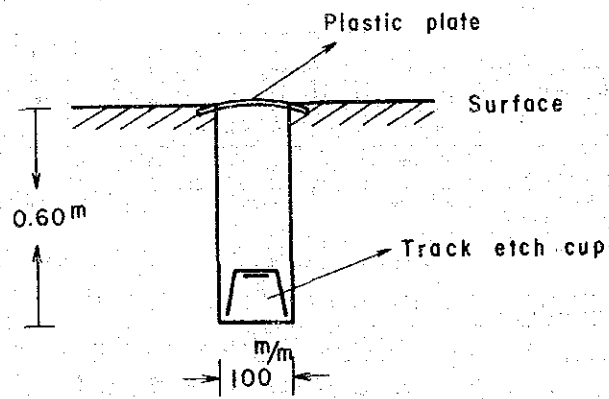


Fig. III-2-2 Planting of Track Etch Cup

Point Sample No.	Date		Rn. cup recovered	Nos. of Days Exposed	Rn. Cup No.	Cup Recovered		Temperature (°C)		Sample Appearance							Geology	Topography				Vegetation								
	measure-ment of 1m depth temp.					fine	disturbed	dirty	dewed	submerged	ambient	bottom (60cm-depth) /m-depth	black	blackish brown	brown	reddish brown		yellowish brown	Wet	intermediate	dried	many	few	none	sandy	clayey	elevation (m)	flat	moderate	steep
21	Oct. 7. 83 11:01		Nov. 3. 83	27	566358				28.2	26.0/25.5													950				SW			
22	Oct. 24. 83 11:50		Nov. 17. 83	24	566482				27.3	24.0/24.6													910				NW			
23	Oct. 24. 83 12:45		Nov. 17. 83	24	566484				29.3	29.6/24.2													950				W			
24	Oct. 24. 83 13:55		Nov. 17. 83	24	566485				28.5	22.5/22.2													970				NW			
25	Oct. 10. 83 11:00		Nov. 4. 83	25	566381				25.2	21.8/22.0													1185				NE			
26	Oct. 10. 83 10:40		Nov. 4. 83	25	566380				23.6	22.8/23.2													1225				N			
27	Oct. 10. 83 10:00		Nov. 4. 83	25	566377				24.7	24.0/24.9													1320				N			
28	Oct. 10. 83 9:40		Nov. 4. 83	25	566376				24.0	23.0/23.1													1350				N			
29	Oct. 10. 83 9:00		Nov. 4. 83	25	566374				20.1	21.6/21.5													1380				W			
30	Oct. 18. 83 8:32		Nov. 9. 83	22	566426				24.6	23.2/23.7													910				N			
31	Oct. 6. 83 12:58		Nov. 2. 83	27	566370				29.6	24.0/24.2													960				S			
32	Oct. 17. 83 9:40		Nov. 8. 83	22	566421				28.3	26.7/26.7													1010				E			
33	Oct. 17. 83 9:58		Nov. 8. 83	22	566422				32.7	25.4/25.4													980				S			
34	Oct. 7. 83 11:30		Nov. 3. 83	27	566359				29.0	24.0/24.2													890				SW			
35	Oct. 10. 83 13:25		Nov. 4. 83	25	566386				28.7	24.3/25.3													1000				NE			
36	Oct. 10. 83 13:10		Nov. 4. 83	25	566385				31.7	25.7/25.4													1050				NE			
37	Oct. 10. 83 11:35		Nov. 4. 83	25	566383				27.7	24.2/23.6													1100				NE			
38	Oct. 10. 83 11:15		Nov. 4. 83	25	566382				28.0	22.8/22.7													1140				NE			
39	Oct. 10. 83 10:30		Nov. 4. 83	25	566379				26.1	23.1/23.0													1240				N			

⊙ : common ○ : little

⊗ : much

Point Sample No.	Date		Rn. cup recovered	No. of Days Exposed	Rn. Cup No.	Cup Recovered				Temperature (°C)		Sample Appearance				Geology	Topography				Vegetation							
	measure-ment of 1m depth temp.					fine	disturbed	dirty	dewed	submerged	ambient	bottom (60cm-depth)/1m-depth	black	blackish brown	brown		reddish brown	yellowish brown	wet	intermediate	dried	many	few	none	sandy	clayey	elevation (m)	Slope
40	Oct. 10. 83	10:20	Nov. 4. 83	25	566378					24.1	24.6/24.6	black											1270	flat		⊙	⊙	
41	Oct. 10. 83	9:21	Nov. 4. 83	25	566375					23.6	23.3/23.3	blackish brown	○										1340	moderate	E	⊙	⊙	
42	Oct. 18. 83	9:25	Nov. 9. 83	22	566427	○				33.4	26.4/26.2	blackish brown	○										840	moderate	E	⊙	⊙	
43	Oct. 6. 83	13:34	Nov. 2. 83	27	566372					32.8	26.4/26.2	blackish brown		○									920	moderate	N	⊙	⊙	
44	Oct. 6. 83	13:19	Nov. 2. 83	27	566371					28.2	23.9/23.2	blackish brown		○									930	moderate	N	⊙	⊙	
45	Oct. 17. 83	10:30	Nov. 8. 83	22	566423	○				30.4	25.0/25.4	blackish brown											900	moderate	SE	⊙	⊙	
46	Oct. 17. 83	11:30	Nov. 8. 83	22	566425					23.2	23.5/23.2	blackish brown											810	moderate	S	⊙	⊙	
47	Oct. 7. 83	12:00	Nov. 3. 83	27	566360					29.8	24.2/ -	blackish brown											860	moderate	SE	⊙	⊙	
48	Oct. 14. 83	13:51	Nov. 8. 83	25	566437	○				27.8	23.4/23.9	blackish brown											880	moderate	W	⊙	⊙	
49	Oct. 14. 83	13:05	Nov. 8. 83	25	566435					28.2	23.6/24.0	blackish brown											910	moderate	NE	⊙	⊙	
50	Oct. 14. 83	12:25	Nov. 8. 83	25	566433	○				30.4	23.0/23.3	blackish brown											910	moderate	N	⊙	⊙	
51	Oct. 14. 83	11:30	Nov. 8. 83	25	566432	○				28.8	23.7/23.8	blackish brown											950	moderate	W	⊙	⊙	
52	Oct. 24. 83	9:25	Nov. 17. 83	24	566467	○				26.1	23.2/23.9	blackish brown											1105	moderate	N	⊙	⊙	
53	Oct. 14. 83	10:03	Nov. 8. 83	25	566399					28.8	22.6/23.0	blackish brown											1080	moderate	NE	⊙	⊙	
54	Oct. 14. 83	9:30	Nov. 8. 83	25	566398	○				25.9	22.7/22.9	blackish brown											1110	moderate	N	⊙	⊙	
55	Oct. 18. 83	9:47	Nov. 18. 83	22	566428	○				29.9	23.1/ -	blackish brown											780	moderate	NE	⊙	⊙	
56	Oct. 6. 83	13:51	Nov. 2. 83	27	566373					27.0	22.9/23.4	blackish brown											900	moderate	NE	⊙	⊙	
57	Oct. 18. 83	11:51	Nov. 9. 83	22	566443	○				31.0	24.5/24.6	blackish brown											855	moderate	SE	⊙	⊙	
58	Oct. 18. 83	12:11	Nov. 9. 18	22	566444	○				33.4	25.0/24.8	blackish brown											830	moderate	SE	⊙	⊙	

⊙ : much ○ : common × : little

Point Sample No.	Date		Rn. cup recovered	Nos. of Days Exposed	Rn. Cup No.	Cup Recovered				Temperature (°C)		Soil Colour				Sample Appearance				Topography			Vegetation							
	measure-ment of 1m depth temp.					fine	disturbed	dirty	dewed	submerged	ambient	bottom (60cm-depth) / 1m-depth	black	blackish brown	brown	reddish brown	yellowish brown	wet	intermediate	dried	many	few	none	sandy	clayey	elevation (m)	flat	moderate	steep	dipping
59	Oct. 17. 83 10:47	Nov. 8. 83		22	566424					32.7	25.3/25.6												820			S	⊙			
60	Oct. 12. 83 13:25	Nov. 12. 83		26	566410					27.0	26.0/26.4												960			N	⊙			
61	Oct. 14. 83 13:35	Nov. 14. 83		25	566436					28.5	23.9/24.5												910			E	⊙			
62	Oct. 14. 83 12:55	Nov. 14. 83		25	566434					29.3	23.4/23.6												920			W	⊙			
63	Oct. 24. 83 8:55	Nov. 17. 83		24	566465					24.3	22.3/22.4												1190			E	⊙			
64	Oct. 24. 83 9:15	Nov. 17. 83		24	566466					31.6	23.2/23.2												1100			E	⊙			
65	Oct. 14. 83 10:45	Nov. 14. 83		25	566431					29.1	23.3/23.3												1000			E	⊙			
66	Oct. 14. 83 10:25	Nov. 14. 83		25	566400					26.3	23.3/23.9												1030			N	⊙			
67	Oct. 19. 83 8:30	Nov. 9. 83		21	566445					26.7	25.6/27.4												800			S	⊙			
68	Oct. 18. 83 11:31	Nov. 9. 83		22	566442					27.7	23.6/23.7												380			N	⊙			
69	Oct. 18. 83 11:19	Nov. 9. 83		22	566441					28.7	24.3/24.7												870			E	⊙			
70	Oct. 12. 83 14:15	Nov. 7. 83		26	566412					25.0	23.6/24.6												850			N	⊙			
71	Oct. 12. 83 13:50	Nov. 7. 83		26	566411					24.2	24.3/25.1												900			N	⊙			
72	Oct. 12. 83 13:05	Nov. 7. 83		26	566409					29.0	22.9/25.5												1010			N	⊙			
73	Oct. 12. 83 12:50	Nov. 7. 83		26	566408					22.9	22.9/23.1												1070			N	⊙			
74	Oct. 12. 83 12:35	Nov. 7. 83		26	566407					24.0	23.1/23.4												1200			N	⊙			
75	Oct. 12. 83 12:10	Nov. 7. 83		26	566405					25.3	22.8/22.9												1210			N	⊙			
76	Oct. 12. 83 11:20	Nov. 7. 83		26	566404					22.9	22.3/22.7												1100			SW	⊙			
77	Oct. 14. 83 9:10	Nov. 8. 83		25	566397					23.8	23.6/24.5												1040			SE	⊙			

⊙ : much ○ : common × : little

Point Sample No.	Date		Nos. of Days Exposed	Rn. Cup No.	Cup Recovered				Temperature (°C)		Sample Appearance								Geology	Topography			Vegetation						
	measure-ment of 1m depth temp.	Rn cup recovered			fine	disturbed	dirty	dewed	submerged	ambient	bottom (60cm depth)	black	blackish brown	brown	reddish brown	yellowish brown	wet	intermediate		dried	many	few	none	Grain size	elevation (m)	flat	moderate	steep	dipping
97	Oct. 12.83 10:15	Nov. 7.83	25	566390					27.8	24.0/24.4													1250			SE			
98	Oct. 12.83 9:40	Nov. 7.83	25	566388					19.9	22.2/22.6													1325			N			
99	Oct. 20.83 8:55	Nov. 10.83	23	566457					30.8	25.8/25.7													890			SE			
100	Oct. 19.83 9:05	Nov. 9.83	25	566447					30.5	24.7/25.1													800			S			
101	Oct. 19.83 10:10	Nov. 9.83	21	566449					27.5	21.9/22.1													790			E	X		
102	Oct. 28.83 11:23	Nov. 21.83	21	566542					24.6	25.0/25.2													950			N			
103	Oct. 28.83 11:05	Nov. 21.83	21	566541					24.9	23.9/24.1													950			N			
104	Oct. 28.83 10:50	Nov. 21.83	23	566480					24.5	23.5/23.9													990			NE			
105	Oct. 28.83 10:35	Nov. 21.83	23	566479					26.4	22.5/22.5													1040			N			
106	Oct. 28.83 10:15	Nov. 21.83	23	566478					24.6	22.8/24.1													1150			N			
107	Oct. 13.83 10:44	Nov. 7.83	23	566420					23.3	24.0/24.6													1250			NW			
108	Oct. 13.83 9:56	Nov. 7.83	23	566417					21.6	24.0/24.4													1240			E			
109	Oct. 13.83 9:45	Nov. 7.83	23	566416					21.5	22 /22.6													1260			NE			
110	Oct. 13.83 9:15	Nov. 7.83	23	566414					22.4	22.0/22.5													1335			NE			
111	Oct. 13.83 8:20	Nov. 7.83	25	566413					22.2	23.6/24.2													1350			NE			
112	Oct. 20.83 9:10	Nov. 10.83	21	566458					23.5	27.2/24.2													895			SE	X		
113	Oct. 19.83 9:30	Nov. 9.83	21	566448					27.4	24.2/ -													800			SW			
114	Oct. 19.83 11:55	Nov. 9.83	21	566451					27.6	22.9/23.1													780			NE			
115	Oct. 19.83 12:20	Nov. 9.83	21	566452					28.9	25.4/24.3													770			NE			

⊙ : much ○ : common × : little

Point Sample No.	Date		Nos. of Days Exposed	Rn. Cup No.	Cup Recovered				Temperature (°C)		Sample Appearance							Topography			Vegetation				
	measure-ment of lm depth temp.	Rn. cup recovered			fine	disturbed	dirty	dewed	submerged	ambient	bottom 60cm-depth /lm-depth	Soil Colour	Humidity	Block	Grain size	Geology	elevation (m)	flat	moderate	steep	dipping	suniness	forestal	grassv	naked rock
154	Oct. 19. 83 12:52	Nov. 9. 83	21	566454	○				32.3	25.9/27.1	black														
155	Oct. 24. 83 9:35	Nov. 17. 83	24	566468	○				31.2	24.6/ -	blackish brown														
156	Oct. 24. 83 10:20	Nov. 17. 83	24	566469	○				32.4	23.5/23.7	blackish brown														
157	Oct. 24. 83 10:45	Nov. 17. 83	24	566470	○				31.5	22.7/23.4	blackish brown														
158	Oct. 24. 83 12:35	Nov. 17. 83	24	566483	○				28.3	22.7/22.8	blackish brown														
159	Oct. 25. 83 10:05	Nov. 17. 83	23	566490	○				31.3	23.2/23.8	blackish brown														
160	Oct. 25. 83 10:45	Nov. 17. 83	23	566492	○				32.4	22.6/23.5	blackish brown														
161	Oct. 26. 83 9:05	Nov. 18. 83	23	566502	○				31.0	24.3/24.6	blackish brown														
162	Oct. 26. 83 11:10	Nov. 18. 83	23	566509	○				28.5	23.7/25.4	reddish brown														
163	Oct. 27. 83 9:10	Nov. 18. 83	22	566472	○				23.0	22.4/23.4	reddish brown														
164	Oct. 27. 83 9:35	Nov. 18. 83	22	566473	○				27.0	23.8/24.5	reddish brown														
165	Oct. 27. 83 10:05	Nov. 18. 83	22	566474	○				26.3	22.6/23.1	reddish brown														
166	Oct. 27. 83 10:25	Nov. 18. 83	22	566475	○				27.6	22.7/23.4	reddish brown														
167	Oct. 28. 83 11:35	Nov. 21. 83	24	566543	○				24.3	22.3/22.7	reddish brown														
168	Oct. 31. 83 10:24	Nov. 19. 83	19	566521	○				29.3	25.8/26.2	blackish brown														
169	Oct. 31. 83 10:38	Nov. 19. 83	19	566522	○				28.8	26.4/26.4	blackish brown														
170	Oct. 31. 83 10:35	Nov. 19. 83	19	566548	○				32.2	24.8/21.9	blackish brown														
171	Oct. 31. 83 10:55	Nov. 19. 83	19	566549	○				27.9	23.9/24.4	blackish brown														
172	Oct. 31. 83 11:05	Nov. 19. 83	19	566550	○				31.7	26.3/26.0	blackish brown														

○ : much ○ : common × : little

Point Sample No.	Date		Nos. of Days Exposed	Rn. Cup No.	Cup Recovered				Temperature (°C)		Sample Appearance								Geology	Topography			Vegetation							
	measure-ment of 1m depth temp.	Rn. cup recovered			fine	disturbed	dirty	dewed	submerged	ambient	bottom (60cm-depth)	black	blackish brown	brown	reddish brown	yellowish brown	wet	intermediate		dried	Humidity	Block	Grain size	elevation (m)	flat	moderate	steep	sunniness	forestal	grassy
173	Oct. 31. 83 11:35	Nov. 19. 83	19	566531	○				35.7	25.2/25.4																				
174	Oct. 31. 83 11:45	Nov. 19. 83	19	566532		○			31.3	27.1/27.1																				
175	Oct. 31. 83 12:00	Nov. 19. 83	19	566533		○			33.4	27.1/27.4																				
176	Oct. 31. 83 12:10	Nov. 19. 83	19	566534		○			31.4	27.9/27.7																				
177	Oct. 31. 83 12:35	Nov. 19. 83	19	566535		○			29.5	26.4/26.4																				
178	Oct. 31. 83 10:50	Nov. 19. 83	19	566523		○			28.8	24.8/25.5																				
179	Oct. 31. 83 11:35	Nov. 19. 83	19	566524		○			34.0	26.8/26.8																				
180	Oct. 31. 83 12:50	Nov. 19. 83	19	566525		○			31.1	25.0/25.0																				
181	Oct. 31. 83 13:00	Nov. 19. 83	19	566526		○			28.3	25.5/25.8																				
182	Oct. 31. 83 13:27	Nov. 19. 83	19	566527		○			33.1	25.1/25.6																				
183	Oct. 31. 83 13:40	Nov. 19. 83	19	566528		○			30.5	27.3/27.9																				
184	Nov. 3. 83 8:30	Nov. 21. 83	18	566529		○			24.0	22.0/22.4																				
185	Nov. 3. 83 8:45	Nov. 21. 83	18	566530		○			26.6	25.5/25.3																				
186	Nov. 3. 83 8:55	Nov. 21. 83	18	566536		○			27.8	26.4/26.3																				
187	Nov. 3. 83 9:40	Nov. 21. 83	18	566538		○			26.6	22.8/23.0																				
188	Nov. 3. 83 10:00	Nov. 21. 83	18	566539		○			27.7	22.9/23.1																				
189	Nov. 3. 83 10:10	Nov. 21. 83	18	566540		○			27.3	23.6/23.8																				
190	Nov. 3. 83 9:20	Nov. 21. 83	18	566537		○			26.1	25.2/25.1																				
191	Nov. 3. 83 10:30	Nov. 21. 83	18	566511		○			26.7	24.7/25.1																				

◎ : much ○ : common X : little

Point Sample No.	Date		Nos. of Days Exposed	Rn. Cup No.	Cup Recovered				Temperature (°C)		Sample Appearance								Geology	Topography				Vegetation								
	measure- ment of lm depth temp.	Rn. cup recovered			fine	disturbed	dirty	dewed	submerged	ambient	bottom 60cm-depth /lm-depth	black	blackish brown	brown	reddish brown	yellowish brown	wet	intermediate		dried	many	few	none	Grain size	elevation (m)	flat	moderate	steep	dipping	suniness	forestal	grassy
192	Nov. 3.83 10:40	Nov. 21.83	18	566512	○				28.7	23.3/23.5	○	○	○	○	○	○	○	○	○	○	○	1000	○	○	○	○	○	○	○	○	○	
193	Nov. 4.83 8:23	Nov. 21.83	17	566513	○				24.8	26.4/25.9	○	○	○	○	○	○	○	○	○	○	○	910	○	○	○	○	○	○	○	○	○	
194	Nov. 4.83 8:40	Nov. 21.83	17	566514	○				22.9	25.6/25.7	○	○	○	○	○	○	○	○	○	○	○	930	○	○	○	○	○	○	○	○	○	
195	Nov. 4.83 9:00	Nov. 21.83	17	566515	○				28.3	24.4/24.7	○	○	○	○	○	○	○	○	○	○	○	950	○	○	○	○	○	○	○	○	○	
196	Nov. 4.83 9:10	Nov. 21.83	17	566516	○			○	27.0	24.6/24.6	○	○	○	○	○	○	○	○	○	○	○	985	○	○	○	○	○	○	○	○	○	
197	Nov. 4.83 9:25	Nov. 21.83	17	566517	○			○	25.0	26.0/25.7	○	○	○	○	○	○	○	○	○	○	○	960	○	○	○	○	○	○	○	○	○	
198	Nov. 4.83 9:35	Nov. 21.83	17	566518	○				27.3	25.4/25.7	○	○	○	○	○	○	○	○	○	○	○	900	○	○	○	○	○	○	○	○	○	○
199	Nov. 4.83 9:50	Nov. 21.83	17	566519	○			○	27.6	24.2/24.3	○	○	○	○	○	○	○	○	○	○	○	850	○	○	○	○	○	○	○	○	○	○
200	Nov. 4.83 10:05	Nov. 21.83	17	566520	○			○	28.3	25.3/25.2	○	○	○	○	○	○	○	○	○	○	○	790	○	○	○	○	○	○	○	○	○	○

◎ : much ○ : common × : little

visible signs or labels were placed to mark the spots in order to facilitate subsequent recovery of the Radon cups. The cup number, date of emplacement and retrieval, and description of the cup when recovered were noted. After three weeks, the radon cups were noted. After three weeks, the radon cups were collected and these were sent to Terradex Corporation for radon track-etch analysis.

2.2.2 O/H Isotope Investigation of Hot Spring Water

A total of fifteen (15) samples were collected from the surface and underground tunnels in the survey area for isotope analysis. 500-ml. bottles were used as sample containers. The bottle was cleaned 2-3 times with the water sample, then filled with the water sample and sealed. The samples were brought back to Japan for O/H isotope analysis at the Central Research Laboratory of Mitsubishi Metal Corporation.

(a) Occurrence of Hot Spring Water: Sampling locations are shown in Fig. III-2-3 and occurrences of discharge are indicated in Table III-2-2. Details of sampling are given below:

(i) No. 1 (Gradient hole AGH-1): The hot water coming from gradient AGH-1 was sampled. The rate of discharge is about 2.5 lit/min., the temperature 66.2°C and pH 7.0. The gradient hole was drilled in andesitic tuff breccia and andesite lava.

(ii) No. 2 (Ambalanga River): The site is located about 300 meters upstream of AGH-1 hole. The geology is composed of light green-colored andesitic tuff breccia cut by andesite dikes. Hot spring water discharges along joint planes. The water flow rate is about 3 lit/min., the temperature 73.8°C and pH 7.0. The host rock is altered and is light green in color. Many calcite veinlets occur.

(iii) Nos. 3, 4 and 5 (2,900 level, Acupan mine): Discharge of hot water is widespread inside the mine workings occurring particularly along the joint planes in Virac granodiorite. The samples were collected on the spots of comparatively

large discharge volume. Three samples have discharge rate of 100 lit/min., 50 lit/min. and 100–150 lit/min., respectively, at corresponding temperatures of 35.9° C, 43.5° C and 41.7° C, and identical pH of 7.0. The host rock is altered and is pale greenish gray in color. Precipitation of calcium sulfate and ferrous iron sulfate is observed.

(iv) No. 6 (3,150 level of Acupan mine): The hot spring water running on the tunnel floor was sampled. It has a flow rate of 5 lit/min., a temperature of 65° C and pH of 7.5. The surrounding rocks are composed of light green andesitic tuff breccia of the old Balatoc plug partially cut by andesite dikes.

(v) No. 7 (3,150 level of Acupan mine): There was difficulty in approaching the exact point of discharge due to extremely heated air. Consequently, the hot water flowing on the tunnel floor was sampled. It has a flow rate of 10 lit/min., a temperature of 90° C and pH of 7.5. The exposed lithology is of dacite volcanic breccia of light green color and tuff breccia. Pervasive pyrite dissemination, silicification and occurrence of calcite veinlets are noted.

(vi) No. 8 (3,150 level of Acupan mine): The sample collected was flowing on the tunnel floor from an area blocked-off from hot air fluid. It has a flow rate of 2 lit/min., a temperature of 65° C and pH of 7.0. Young plugs of pale green dacitic volcanic breccia-tuff breccia comprise of the host rock.

(vii) No. 9 (3,150 level of Acupan mine): Hot water with steam springs out of the D/D drill hole and joint planes and flows down the tunnel floor where it was sampled. It has a flow rate of about 70 lit/min., a temperature of 75° C and pH of 7.5. The host rock is pale greenish gray andesitic tuff breccia representing the boundary of the old and young plugs.

(viii) Nos. 10 and 11 (3,150 level of Acupan mine): The sample collected was hot water flowing down the tunnel floor from the joints of the roof and wall of the tunnel. It has a flow rate of 50–60 lit/min., a temperature of 80° C and pH of 7.0–7.5. The nearby host rock is granodiorite of whitish gray-white in color. Intense silicification is observed. No. 10 site comprises of andesite intrusive of green-dark green color.

(ix) Nos. 12 and 13 (3,300 level of Acupan mine): Inside the tunnel, the temperature was as high as 65°C. Steam and thermal fluid gushes out from the drill hole. The tunnel is blocked immediately before the site of the spring in order to prevent the circulation of hot air. The sample collected was thermal fluid running in the drain. The flow rates of the two samples are 25–30 lit/min., the temperatures are 57.1°C and 85.8°C, and pH 7.0 and 7.5 for No. 12 and 13, respectively.

The nearby host rock is composed of pale green andesitic tuff breccia and is cut by andesite dikes. Amphibole is altered to chlorite. Strong pyrite dissemination and silicification are observed. Abundant white calcium sulfate deposits occur on the vent pipes installed adjacent to the rocks.

(x) No. 14 (2,300 level of Acupan mine): The sample collected was thermal fluid flowing down the floor tunnel from the tunnel wall. It has a flow rate of 50–100 lit/min., a temperature of 32.8°C and pH of 7.0. The host rock is composed of pale green dacitic volcanic tuff breccia.

(xi) No. 15 (700 meter above sea level, Acupan mine): A drain tunnel was constructed at a site about 100 meters northwest from the AGH-1 drill hole. The hot spring water was sampled from the tunnel wall, and has a discharge rate of about 5 lit/min., a temperature of 73.1°C and pH of 7.5. The lithology of the host rock is green-colored andesitic breccia.

(b) O/H Isotope Analysis: For hydrogen and oxygen, the isotopic ratio may be expressed as deviation in per mil (part per thousand) to a reference material as given below.

$$\delta X = \left[\frac{R. \text{ sample}}{R. \text{ standard}} - 1 \right] \times 1,000$$

where X denotes D, ^{18}O ; R. sample and R. standard represent, respectively, the D/H and $^{18}\text{O}/^{16}\text{O}$ of the sample and the standard material. SMOW (Standard Mean Ocean Water) is used as standard material for hydrogen and oxygen.

Hydrogen is generated by allowing the sample water to react with metallic uranium which is heated to about 800°C in a vacuum unit. The dissolved hydrogen is collected by means of Teopler pump and D/H ratio is determined using isotope analyzer (RMS-HB) of Hitachi Ltd. after measurement of rate recovery. In the case of oxygen, the sample waters and carbon dioxide are set in vacuum container, which is kept shaking in a water tank at a constant temperature of 25°C for one day and overnight. In this way, water and carbon dioxide reach the isotopic exchange equilibrium for $^{18}\text{O}/^{16}\text{O}$, and the isotopic ratio of water is measured in comparison with $^{18}\text{O}/^{16}\text{O}$ ratio of carbon dioxide. The measuring instrument is the mass spectrometer, Micromass 903 of VG Isotope, Ltd.

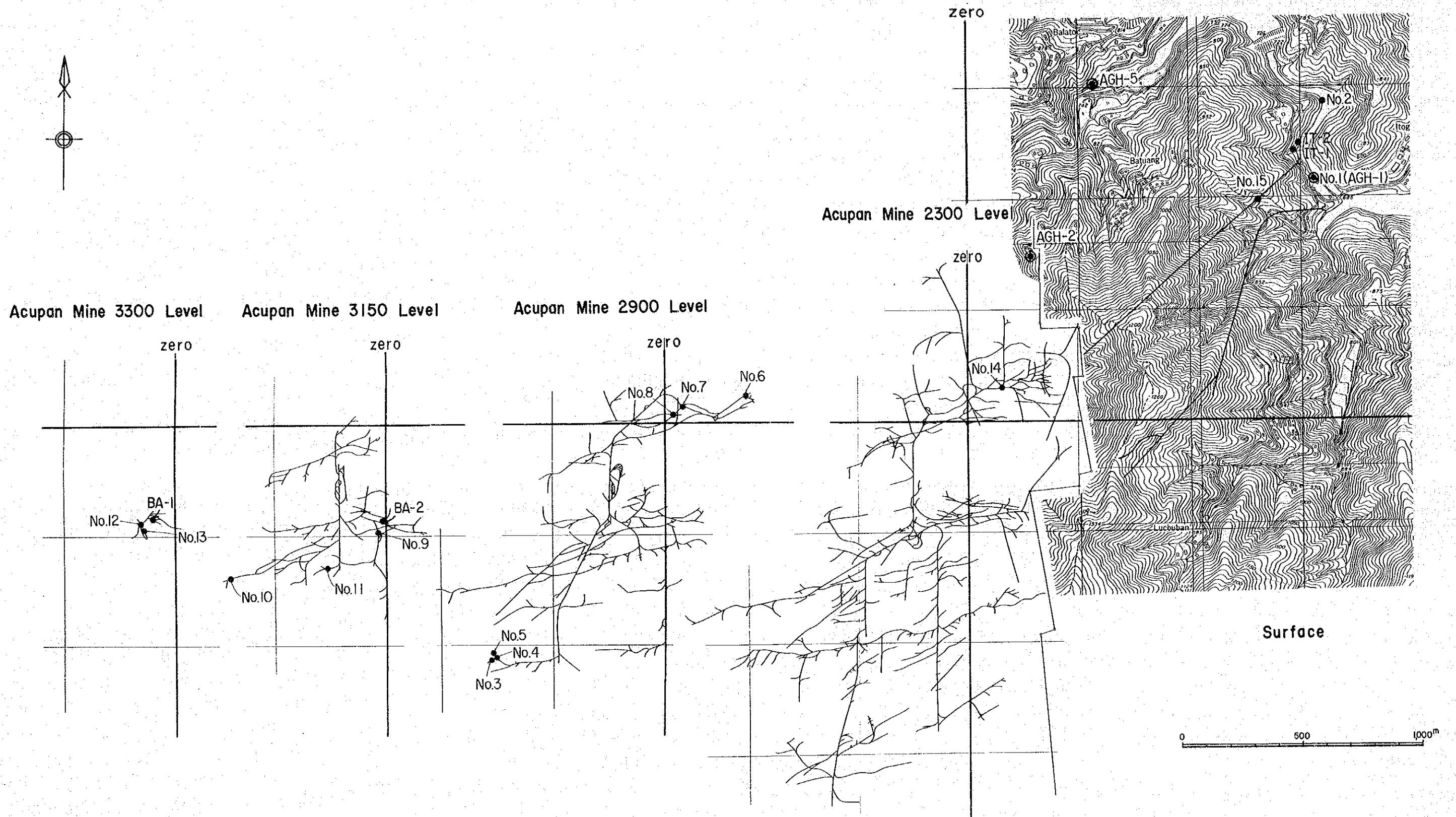


Fig. III-2-3 Location Map of Water Spring